Proc. Natl. Acad. Sci. USA
Vol. 91, pp. 10680–10684, October 1994
Immunology

Identification of the complement iC3b binding site in the β2 integrin CR3 (CD11b/CD18)

(adhesion molecules/reperfusion injury/complement activation/inflammation)

TAKEO UEDA, PHILIPPE RIEU, JAMES BRAYER, AND M. AMIN ARNAOUT*

Leukocyte Biology and Inflammation Program, Department of Medicine, Massachusetts General Hospital and Harvard Medical School, Boston, MA 02129

Communicated by Dr. Eugene Braunwald, June 6, 1994 (received for review March 18, 1994)

ABSTRACT The divalent cation-dependent interaction of the β2 integrin CR3 (CD11b/CD18) with the major complement opsonic C3 fragment iC3b is an important component of the central role of CR3 in inflammation and immune clearance. In this investigation we have identified the iC3b binding site in CR3. A recombinant fragment representing the CR3 A-domain, a 200-amino acid region in the ectodomain of the CD11b subunit, bound to iC3b directly and in a divalent cation-dependent manner. The iC3b binding site was further localized to a short linear peptide that also bound iC3b directly and inhibited iC3b binding to the A-domain as well as to CR3 expressed by human neutrophils. These data establish a major recognition function for the integrin A-domain and have important implications for development of novel antiinflammatory therapeutics.

Neutrophil extravasation into tissues and phagocytosis of complement-coated particles are essential steps in host defense against infections. These processes have the potential, however, of inflicting serious tissue injury in many noninfectious diseases such as myocardial infarction, burns, hemorrhagic shock, autoimmune disorders, and allograft rejection (reviewed in ref. 1). Complement receptor type 3 (CR3, CD11b/CD18, Mo-1, Mac-1) is a major cell surface glycoprotein used by circulating phagocytes to migrate into inflamed organs and to phagocytose opsonized particles (reviewed in ref. 1). CR3, a member of the β2 integrins, is a heterodimer consisting of two noncovalently associated subunits CD11b and CD18, with apparent molecular masses of 160 kDa and 94 kDa, respectively. The CD18 subunit is shared by two other subunits, CD11a and CD11c, comprising, respectively, the CD11a/CD18 (LFA-1, TA-1) and CD11c/CD18 (p150,95, Leu-M5) heterodimers (reviewed in ref. 1). Inherited deficiency of β2 integrins (Leu-CAM deficiency) compromises the phagocytic and migratory capacities of circulating granulocytes and monocytes, leading to life-threatening bacterial infections (1). Monoclonal antibodies (mAbs) to the CD11b or CD18 subunits of CR3 reproduce these defects in experimental animals, underscoring the major role of CR3 in these events.

CR3 interacts in a divalent cation-dependent manner with several ligands, the best characterized being the complement C3 fragment iC3b (reviewed in ref. 1). iC3b is a heterodimeric serum-derived glycoprotein of 180 kDa that is generated upon activation of the classical or alternative complement pathways (2). Complement activation rapidly leads to the proteolytic cleavage of serum C3 and the covalent binding of its largest fragment, C3b, to the activating surface. In serum, surface-bound C3b has a half-life of ≈90 sec, due to its rapid cleavage into iC3b by the specific serine proteinase, factor I. The significantly longer half-life of iC3b (≈35 min) suggests that it is the major C3 fragment mediating immune clearance *in vivo* (3). Inherited deficiency of factor I (4) prevents the generation of iC3b and predisposes to recurrent bacterial infections, reflecting the important biologic and pathologic functions of CR3–iC3b interactions.

Progress in understanding the structural basis for the interaction of CR3 with iC3b has been hampered by the large size of the receptor and the ligand, their multi-subunit composition, the unstable nature of iC3b *in vitro*, and the relatively low affinity of fluid-phase monomeric iC3b for CR3. Recently, the epitopes for several anti-CR3 mAbs that inhibit CR3 binding to protein ligands including iC3b were mapped to a unique 200-amino acid divalent cation binding peptide within the extracellular region of CD11b referred to as the A- (or I) domain (5, 6), suggesting that this domain either is directly involved in or is necessary for binding of CR3 to its ligands. We now show that a recombinant (r) form of the CD11b A-domain expressed in *Escherichia coli* binds directly and specifically to iC3b. This binding is divalent cation dependent, as in whole CR3, but differs in being temperature independent. Furthermore, we have mapped the major iC3b binding site to a linear peptide, 14 amino acids in length within the A-domain. Interaction of this peptide with iC3b did not require divalent cations, suggesting that the primary role of divalent cations in the integrin A-domain is to maintain its structural and therefore functional integrity.

MATERIALS AND METHODS

Reagents and Antibodies. Restriction and modification enzymes were bought from New England Biolabs, Boehringer Mannheim, or BRL. The murine mAbs to human CD11b, 44, 903, 904, and OKM9 (5), and to CD11a, TS1/22 (7), have been described. A polyclonal antibody to human CR1 was the kind gift of G. Ross (3).

Generation and Purification of CD11 A-Domain r Proteins. Generation of the CD11b A-domain has been described (5). To generate the CD11a A-domain, the respective cDNA was cloned by PCR using CD11a cDNA-based oligonucleotides (8), inserted in-frame into the *Bam*HI–*Sma* I restricted pGEX-2T vector (Pharmacia), and the ligated product was purified and used to transform *E. coli* JM109 (9). Individual bacterial clones containing the cloned cDNA fragment were identified by restriction analysis, and the recombinant protein was expressed as a glutathione *S*-transferase (GST) fusion protein, purified and released by thrombin (5), and analyzed on denaturing 12% polyacrylamide gels (10).

Synthetic Peptides. Peptides were obtained commercially and purified on HPLC. Selective ones were subjected to amino acid analysis.

Complement C3-Coated Erythrocytes (E). E coated with rabbit anti-E IgM (EA) or C3b (EAC3b) were prepared as

The publication costs of this article were defrayed in part by page charge payment. This article must therefore be hereby marked "*advertisement*" in accordance with 18 U.S.C. §1734 solely to indicate this fact.

Abbreviations: mAb, monoclonal antibody; r, recombinant; GST, glutathione *S*-transferase; E, erythrocyte(s).
*To whom reprint requests should be addressed.

described (11). EAiC3b were generated by treating EAC3b with purified human factors H and I (11) or, alternatively, prepared from EA using C5-deficient human serum (Sigma). EAiC3b cells were washed and stored in isotonic veronal-buffered saline (VBS^{2+}, pH 7.4) containing 1 mM magnesium/0.15 mM calcium ($MgCl_2/CaCl_2$) and 1 mg of soybean trypsin inhibitor per ml (Worthington) at 1.5×10^8 cells per ml. EA, EAC3b, or EAiC3b was labeled with 5- (and-6)-carboxy fluorescein (Molecular Probes) as described (5).

Immobilization of r Proteins and Peptides. Purified rA-domain was added to Immulon-2 96-well microtiter plates (Dynatech) overnight. Wells were then washed once with phosphate-buffered saline (pH 7.4) without metals and blocked with 1% bovine serum albumin at room temperature for 1 hr, followed by two washings with buffer A (60% $GVBS/VBS^{2+}$ mixed in a 1:3 ratio) (5) containing 1 mM $MnCl_2$ or $MgCl_2/CaCl_2$. All peptides were stocked at 1 mg/ml in water and similarly adsorbed to Immulon-2 96-well plates. Binding of the anti-CD11b mAbs to the coated rA-domain was measured by ELISA and read using a plate reader (Molecular Dynamics).

E Binding Assays. Fluoresceinated EAiC3b, EAC3b, or EA was resuspended to 1.5×10^8 per ml in buffer A and added (30 μl) to wells containing immobilized proteins or peptides in a total volume of 100 μl. The plates were then briefly centrifuged to settle the E and incubated at 37°C for 15 min in a humidified incubator with 5% CO_2. For the inhibition studies, E were preincubated with each r protein or pure peptide in the presence of 2% bovine serum albumin for 5 min at room temperature and added to wells coated with immobilized protein or peptide without washing, unless otherwise indicated. At the end of the binding reactions, wells were washed, examined briefly by light microscopy, and then solubilized with 1% SDS/0.2 M NaOH. Fluorescence was quantified (excitatory wavelength, 490 nm; emission wavelength, 510 nm) using a SLM 8000 fluorometer (SLM Aminco, Urbana, IL) (5). In experiments in which the effects of individual divalent cations were measured, Ca^{2+} and Mg^{2+} were replaced with metal-free buffers or with buffers containing each cation at 1 mM. The effect of temperature was evaluated in the presence of 1 mM $MnCl_2$ at 37°C and at 4°C.

Purification and Adherence of Human Neutrophils. Neutrophils were purified as described (12), resuspended in divalent cation-free Tris·HCl/saline buffer (pH 7.4) at 5×10^7 per ml, and kept on ice until used. Neutrophils (2×10^5 cells per well) were allowed to adhere to 96-well plates in Iscove's modified medium for 1 hr at 37°C, in a humidified incubator with 5% CO_2. The wells were then washed, and 5 μl of fluoresceinated EAiC3b or EA (at 1.5×10^8 per ml) was added in the presence of 3% bovine serum albumin, in a total volume of 50 μl, followed by 15 min of incubation at 37°C with 5% CO_2. Wells were then washed and fluorescence was quantified as described above.

Flow Cytometry. Fifteen microliters of EAiC3b or EA (each at 1.5×10^8 per ml) was incubated with 15 μg of biotinylated A7 or control peptides in 100 μl of buffer A containing 1 mM $MnCl_2$ at room temperature for 10 min and washed once. Streptavidin-conjugated phycoerythrin (Sigma) was added to the cell suspension at 1 μg/ml and incubated for 15 min at room temperature. Washed E were then analyzed by a fluorescence-activated cell sorter from Becton Dickinson.

RESULTS AND DISCUSSION

The CD11b A-Domain Contains an iC3b Binding Site. A recombinant CD11b A-domain (Fig. 1) immobilized onto 96-well microtiter plates bound directly and specifically to fluoresceinated EAiC3b (Fig. 2). Binding increased progressively as a function of the concentration of the soluble A-domain used to coat the microtiter wells (Fig. 2*A*), binding was optimal with the addition of 20 μg of A-domain (Fig. 2*A*) and 30 μl of EAiC3b (at 1.5×10^8 per ml) per well, and binding was visible by the naked eye (not shown). Binding was competitively inhibited by fluid-phase A-domain (Fig. 2*B*), with half-maximal inhibition observed at $\approx$1 μM. EAiC3b did not bind to GST (Fig. 2*B*) or to the CD11a A-domain (Fig. 2*C*), and binding was blocked by an anti-CD11b mAb that normally blocks EAiC3b binding to cell-bound CR3 (Fig. 2*D*).

FIG. 1. (*A*) Schematic of a $\beta2$ integrin (1). The amino acid residues comprising the beginning and end of the CD11b and CD11a A-domains are indicated in the native as well as the recombinant forms after thrombin cleavage. Italicized residues are bacterially derived. (*B*) ELISA (mean ± SD, $n = 2$, each in duplicate) showing reactivity of anti-CR3 mAbs 44, OKM9, and 904 with rCD11b A-domain (black bars) but not with GST (hatched bars). Negative controls include omission of the primary antibodies (buffer) or binding of the anti-CD11a mAb, TS1/22. (*Inset*) Coomassie stain of an SDS/polyacrylamide gel (12.5%) following electrophoresis of 3 μg of purified rCD11b A-domain, rCD11a A-domain, and GST (shown in lanes 1, 2, and 3, respectively), migrating with apparent molecular masses of 24 kDa, 22 kDa, and 26 kDa, respectively.

Binding of EAiC3b to the rA-Domain Is Divalent Cation Dependent but Temperature Independent. Binding of CR3 to EAiC3b in whole cells is metal and temperature dependent. We therefore examined the divalent cation and temperature dependency of EAiC3b binding to rA-domain. As can be seen in Fig. 3*A*, 1 mM $MnCl_2$, 1 mM $MgCl_2$, or a combination of 1 mM $MgCl_2$/0.15 mM $CaCl_2$ supported this interaction. $CaCl_2$ alone (0.15–1 mM) was ineffective. No specific binding was observed if divalent cations were omitted or when EDTA was included in the reaction mixture. Similarly, a single point mutation (D242A) that impairs the ability of the rA-domain to bind divalent cations (5) also impaired rA-domain interaction with EAiC3b (Fig. 3*B*).

Binding of EAiC3b to the rA-domain was temperature-independent (Fig. 3*C*). These findings suggest that the r domain may assume a functionally active conformation, lacking in the native CR3 unless the latter is activated by agonists. Posttranslational modifications (14) and conformational changes in the receptors (15) and in the integrin A-domain (16) in response to activation signals have been demonstrated. Alternatively, the temperature dependency of cell-bound CR3–ligand interactions may be explained by temper-

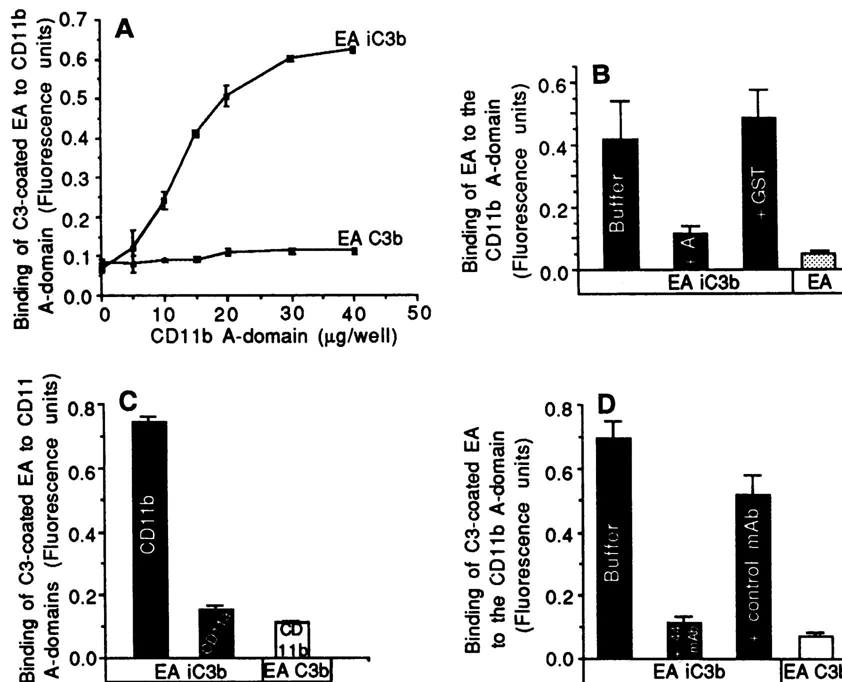

FIG. 2. (*A*) Binding of complement-coated EA to immobilized A-domain as a function of the rA-domain added. Values represent the mean ± SD of three independent experiments each in triplicate. (*B*) Histograms (mean ± SD, $n = 3$) showing the interaction of EAiC3b with adsorbed CD11b A-domain in the absence (buffer) or presence of soluble A-domain (+ A) or GST (+ GST). The background binding of EA is also shown. (*C*) Histograms (mean ± SD, $n = 3$) showing binding of EAiC3b to adsorbed CD11b but not CD11a A-domains. Background binding of EAC3b is shown. (*D*) Histograms (mean ± SD, $n = 3$, each in duplicate) depicting the inhibition of binding of the CD11b A-domain to EAiC3b by the functional murine anti-CR3 mAb 44 (IgG2a) but not by the control mAb 99g (IgG2a) (13). Background binding of EAC3b is shown.

ature-induced clustering of the receptor in the plasma membrane (17), thus facilitating its interaction with ligand, a situation that may be mimicked by using immobilized rA-domain. These two possibilities are not mutually exclusive.

Binding of A-Domain-Derived Peptides to EAiC3b. To further define the region within the A-domain that binds EAiC3b, we used overlapping synthetic peptides spanning the whole A-domain region of CD11b (Fig. 4) and examined the ability of each to bind directly to EAiC3b and to inhibit EAiC3b binding to the A-domain. As can be seen in Fig. 5*A*, two overlapping peptides, AM230 and A24 (calculated pI values of 10.78 and 3.76, respectively), bound directly to EAiC3b but not to EA, and binding was also visible by the naked eye (data not shown). AM230 and A24 comprised most of the sequence encoded by exon 8 of the CD11b gene (18), indicating that the corresponding segment in the protein contains an iC3b binding site. AM230 and A24 had a 14-amino acid overlapping region (Fig. 4). When this region (peptide A7) was synthesized on two separate occasions, adsorbed to plastic, and tested, it bound EAiC3b directly, specifically (Fig. 5*A*), and in a dose-dependent manner (Fig. 5*B*). No binding was observed when a scrambled form of A7 (Sc. A7, Fig. 4) was used (data not shown). Fluid-phase biotinylated A7 also bound directly and specifically to EAiC3b (Fig. 5*C*).

EAiC3b binding to AM230, A24, and A7 was not significantly altered by removal of divalent cations or by inclusion of EDTA (Fig. 5*D* and data not shown). EAiC3b did not bind to wells coated with A7-derived peptides comprising, respectively, the N-terminal half (A9), the C-terminal half (A10), or the smaller C-terminal peptides B21 and B23 (Fig. 5*A*). Microtiter wells precoated with A8, a synthetic peptide from the corresponding A-domain region of CD11a (8), did not bind to EAiC3b (Fig. 5*A*), consistent with the lack of binding of the rCD11a A-domain (Fig. 2*C*) or of rCD11a/CD18 to EAiC3b (not shown). A7 inhibited binding of EAiC3b to the A-domain in a dose-dependent manner, with half-maximal inhibition at 5 μg/ml (≈3.5 μM, or approximately 3- to 4-fold higher than that of the rA-domain) (Fig. 6*A*). At ≥50 μg/ml

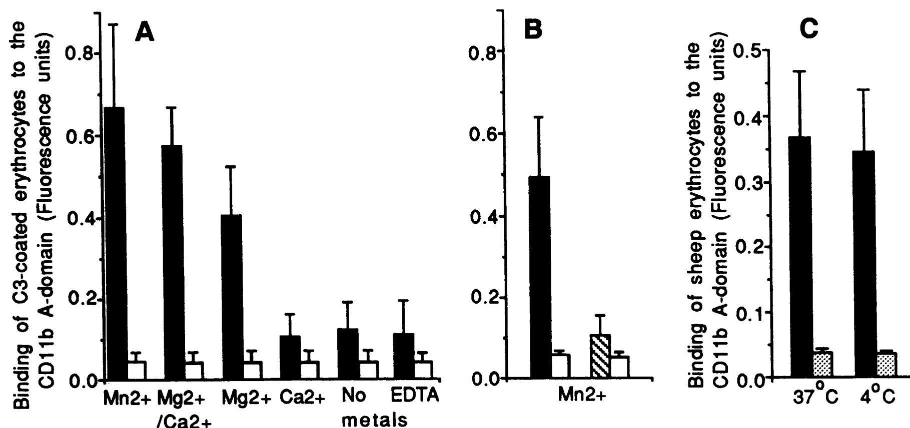

FIG. 3. (*A*) Histograms (mean ± SD, $n = 3$) showing the effects of divalent cations on binding of rCD11b A-domain to iC3b. Binding was measured in the presence of the standard concentration of 1 mM magnesium plus 0.15 mM calcium (Mg^{2+}/Ca^{2+}), in the presence of 1 mM of each divalent cation alone, in the absence of added divalent cations (no metals), and in the presence of 1 mM EDTA. Open bars represent background binding of EAC3b under identical conditions. (*B*) Histograms (mean ± SD, $n = 2$) showing the binding of immobilized wild-type (black bars) and D242A mutant (hatched bars) rCD11b A-domain to EAiC3b in the presence of 1 mM $MnCl_2$. Background binding to EAC3b is also shown (open bars). (*C*) Effect of temperature on the binding of CD11b A-domain to EAiC3b (black bars) or to EA (stippled bars) in the presence of 1 mM $MnCl_2$.

A.

Peptide	Amino acid sequence	Residue No.
A1:	CPQEDSDIAF LIDGSGSIIP	(128–147)
A2:	IIPHDFRRMK EFVSTVMEQL	(145–164)
A3:	EQLKKSKTLF SLMQYSEEFR	(162–181)
A4:	EFRIHFTFKE FQNNPNPRSL	(179–198)
A5:	RSLVKPITQL LGRTHTATGI	(196–215)
A6:	TGIRKVVREL FNITNGARKN	(213–232)
AM230:	KVVRELSNIT NGARKNASKI LVVITDGEK	(217–245)
A24:	NAFKILVVIT DGEKFGDPLG YEDV	(232–255)
A7:	NAFKILVVIT DGEK	(232–245)
A7-BIO.:	*NAFKILVVIT DGEK	(232–245)
A9:	NAFKILV	(232–238)
A10:	VIT DGEK	(239–245)
B21:	DGEKFGDPLG	(242–251)
B23:	DGEKF	(242–246)
B-2:	DGEKFGDPLG YEDVIPEADR	(242–261)
A11:	DREGVIRYVI GVGDAFR	(260–276)
B-5:	FRSEKSRQEL NTIASKPPRD HV	(275–296)
A12:	HVFQVNNFEA LKTIQNQLRE	(295–314)

B.

Peptide	Amino acid sequence	Residue No.
A7M:	NAFKILVVIT aGEK	(232–245)
Sc. A7:	TVDLKFGIKN IEAV	
A8 (CD11a):	DATKVLIIIT DGEA	(229–242)
C392:	QDIVFLIDGS GSISSRNFAT M	(CD11c, 131–151)
Pep.BIO.:	*DMTGAIIEDN YTFLGE	

FIG. 4. (*A*) Names and positions of the overlapping synthetic peptides of CD11b A-domain. (*B*) Control peptides. A7M, a mutant form of A7, with a D → A substitution, indicated by a small letter; Sc. A7, a scrambled form of A7; A8, the corresponding region of CD11a; C392, a CD11c A-domain-derived peptide; Pep. BIO., an irrelevant biotinylated (BIO.) peptide. The biotinylated residue in A7-BIO. and Pep. BIO. is indicated by a star (*). The italicized residues in AM230 indicate position of the two inadvertent substitutions made in this peptide during synthesis.

(35 μM), A7 inhibited EAiC3b binding to the A-domain completely. This inhibition required the continuous presence of A7 and was not secondary to degradation of iC3b or to a toxic effect of this peptide concentration on erythrocytes, since the inhibitory effect was reversible when A7-treated EAiC3b cells were washed prior to their addition to adsorbed rA-domain (data not shown). The ability of each of the remaining peptides to inhibit EAiC3b–rA-domain interaction was then tested at an ≈3-fold higher peptide concentration (200 μg/ml or 100 μM). At this concentration, none of the other tested peptides (including A8 and Sc. A7) significantly inhibited rCD11b A-domain binding to EAiC3b (Fig. 6*B*, and not shown).

The above data do not exclude the possibility that EAiC3b also binds to another site(s) in the CD11b and/or CD18 subunits of CR3. We therefore assessed the ability of A7 to inhibit EAiC3b binding to CR3 expressed by normal human neutrophils, under similar conditions. EAiC3b binding to neutrophils is primarily mediated by CR3 but can also occur *in vitro* through complement receptor type 1 (CR1) (3). The effect of A7 on EAiC3b binding was tested in the presence of blocking concentrations of a polyclonal anti-CR1 antibody. As can be seen in Fig. 6*C*, EAiC3b binding to adherent neutrophils was primarily CR3 mediated under these conditions, since it was inhibited by the anti-CR3 mAb 903, which inhibits iC3b binding selectively (13). A7, but not the control A4, significantly inhibited CR3-dependent binding of EAiC3b to neutrophils with 70% inhibition observed at 100 μM (data not shown) and almost complete inhibition seen at 140 μM (Fig. 6*C*). The ability of A7, AM230, and A24 to bind directly to EAiC3b should now permit the identification of the CR3 recognition site in iC3b (19).

One of the residues involved in coordinating divalent cation binding to the CD11b A-domain is the conserved D242 residue (5). A D242A mutation, where D242 was replaced with alanine, markedly reduced the ability of the rA-domain to bind divalent cations (5) and to bind EAiC3b (Fig. 3*B*). It also impaired the ability of recombinant CR3 to bind EAiC3b (5). D242 is contained within the A7 peptide, yet A7M bound EAiC3b normally, indicating that D242 does not play a direct role in iC3b binding. The likely major function of divalent cations in the A-domain may be to permit formation of a specific, responsive, and flexible three-dimensional structure that allows accessibility of distinct binding sites for protein

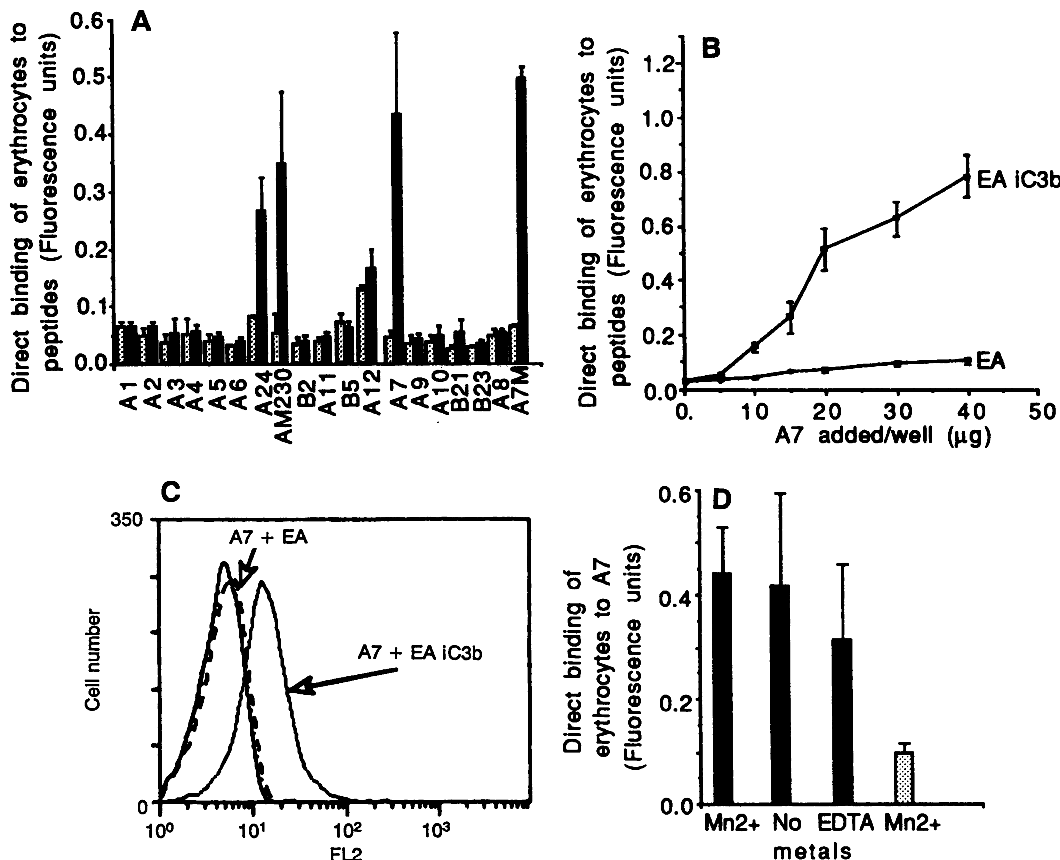

FIG. 5. (*A*) Histograms (mean ± SD, n = 3, each carried out in duplicate) showing binding of iC3b to immobilized synthetic peptides. Background binding of EA to the peptides is also shown (stippled bars). (*B*) Dose–response curves showing the degree of binding of EAiC3b or EA to A7 peptide as a function of the peptide added to each well. (*C*) Direct binding of fluid-phase biotinylated A7 to EAiC3b (wavy) or to EA (dashed). Bound A7 was detected using phycoerythrin-coupled streptavidin and fluorescence-activated cell sorting. Binding of the control peptide (Pep. BIO.) to EAiC3b and to EA is also shown (overshadowed by the negative control tracing). (*D*) Histograms (mean ± SD, n = 3, each in duplicate) showing the effect of $MnCl_2$ on EAiC3b binding to immobilized A7. Binding of EA to A7 (stippled bars) represents background binding.

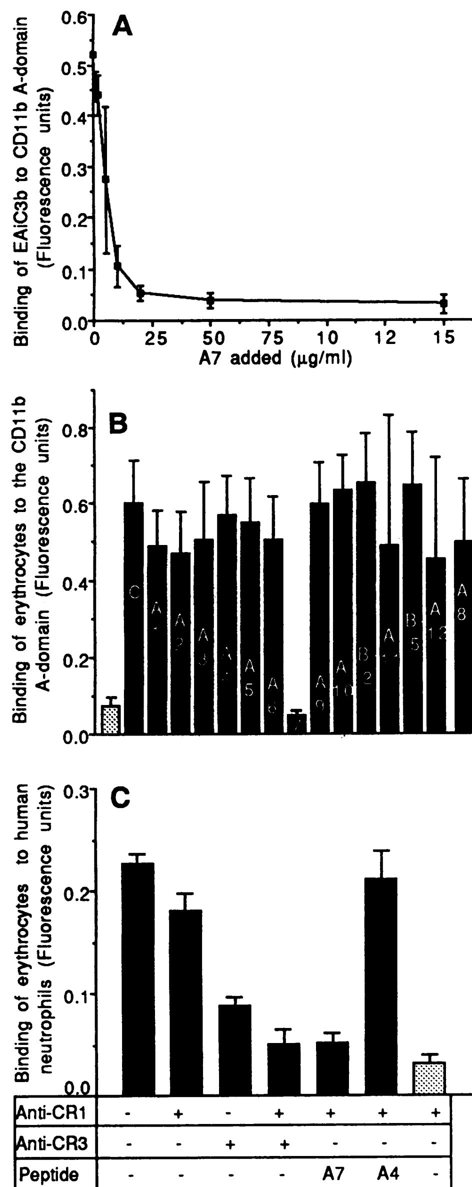

FIG. 6. (*A*) Dose–response curve showing inhibition by A7 of EAiC3b binding to immobilized rCD11b A-domain. Each point represents the mean ± SD of three independent experiments, each done in duplicate. (*B*) Histograms (mean ± SD, $n = 3$) showing the effect of soluble CD11b- and CD11a-derived peptides on EAiC3b binding to immobilized rCD11b A-domain. Binding of EA to the immobilized domain is also shown (stippled bar). (*C*) Inhibition of EAiC3b binding to neutrophil CR3 by A7. Each histogram represents the mean ± SD of two independent experiments, each in duplicate. Peptides were used at a final concentration of 140 μM.

ligands. It is relevant in this regard that different conformational states in the A-domain exist (16) and that native CR3 binding to iC3b in intact cells is markedly up-regulated by agonists (20), suggesting that the protein ligand binding capacity of the A-domain may be altered by inside-out signaling.

The A7 peptide consists of a conserved hydrophobic core flanked by two somewhat less conserved hydrophilic regions. The hydrophobic core (in contrast to its flanking sequences) does not appear to be surface expressed (21). It is likely, therefore, that iC3b binding is contained in residues in the N- and/or C-terminal hydrophilic regions of A7. Detailed mutagenesis of the A7 region, complemented by solution of the three-dimensional structure of the A-domain, will be required for the fine mapping of iC3b contact residues.

CR3 also binds to various ligands that share little structural homology with each other or with iC3b. These include coagulation factors fibrinogen and factor X and the immunoglobulin-like ligand CD54 (ICAM-1) (reviewed in refs. 1 and 22). The mAb OKM9, which binds to the CD11b A-domain directly (Fig. 1*B*), has been reported to block fibrinogen and CD54 binding to CR3 (6, 23), suggesting that the A-domain also contains binding sites for these two ligands. Direct analysis using the respective labeled ligands will be needed to map these sites and relate them to that of iC3b.

The present studies establish the integrin A-domain as an independent structural and functional unit. These data thus lend credence to the hypothesis (reviewed in ref. 24) that the A-domain is an ancient structure that arose by duplication and divergence of a common precursor, which might have served a primordial recognition function and was later incorporated into structurally unrelated proteins, including integrins, to serve specialized functions important in cell adhesion, hemostasis, and inflammation. The present data identify the key role of this domain in the interaction of two major players in cellular and humoral immunity, phagocytic cells and complement, making this domain an excellent target for antiinflammatory drug development. By identifying the iC3b binding site within this domain, the present data make it feasible to develop specific antagonists based on peptidyl analogs or on more advanced homologs, which may be beneficial therapeutically in limiting phagocyte and complement-induced tissue damage that occurs in many immune and inflammatory disorders (1, 22, 25).

We thank Dr. Masahiro Michishita for helpful discussions and Ms. Linda Costa for secretarial assistance. This work was supported by National Institutes of Health Grants DK-48549 and AI-28465, the March of Dimes and Birth Defects Foundation, and an Institut National de la Santé et de la Recherche Médicale fellowship to P.R.

1. Arnaout, M. A. (1990) *Blood* **75**, 1037–1050.
2. Muller-Eberhard, H. J. (1988) *Annu. Rev. Biochem.* **57**, 321–347.
3. Ross, G. D., Cain, J. A. & Lachmann, P. J. (1985) *J. Immunol.* **135**, 2005–2014.
4. Alper, C. A., Abramson, N., Johnston, R. B., Jandle, J. H. & Rosen, F. S. (1970) *J. Clin. Invest.* **49**, 1975–1985.
5. Michishita, M., Videm, V. & Arnaout, M. A. (1993) *Cell* **72**, 857–867.
6. Diamond, M. S., Garcia-Aguilar, J., Bickford, J. K., Corbi, A. L. & Springer, T. A. (1993) *J. Cell Biol.* **120**, 1031–1043.
7. Sanchez-Madrid, F., Nagy, J. A., Robbins, E., Simon, P. A. & Springer, T. A. (1983) *J. Exp. Med.* **158**, 1785–1803.
8. Larson, R. S., Corbi, A. L., Berman, L. & Springer, T. (1989) *J. Cell Biol.* **108**, 703–712.
9. Maniatis, T., Fritsch, E. F. & Sambrook, J. (1989) *Molecular Cloning: A Laboratory Manual* (Cold Spring Harbor Lab. Press, Plainview, NY), 2nd Ed.
10. Laemmli, U. K. (1970) *Nature (London)* **227**, 680–685.
11. Dana, N., Todd, R. F., III, Pitt, J., Springer, T. & Arnaout, M. A. (1984) *J. Clin. Invest.* **73**, 153–159.
12. Boyum, A. (1968) *Scand. J. Clin. Lab. Invest.* **97**, Suppl 77.
13. Dana, N., Styrt, B., Griffin, G. D., Todd, R. F., III, Klempner, M. S. & Arnaout, M. A. (1986) *J. Immunol.* **137**, 3259–3263.
14. Chatila, T., Geha, R. S. & Arnaout, M. A. (1989) *J. Cell Biol.* **109**, 3435–3444.
15. Lo, S. K., Detmers, P. A., Levin, S. M. & Wright, S. D. (1989) *J. Exp. Med.* **169**, 1779–1793.
16. Diamond, M. S. & Springer, T. A. (1993) *J. Cell Biol.* **120**, 545–556.
17. Detmers, P. A., Wright, S. D., Olsen, E., Kimball, B. & Cohn, Z. A. (1987) *J. Cell Biol.* **105**, 1137–1145.
18. Fleming, J. C., Pahl, H. L., Gonzalez, D. A., Smith, T. F. & Tenen, D. G. (1993) *J. Immunol.* **150**, 480–490.
19. Taniguchi, S. A. & Isenman, D. E. (1992) *J. Biol. Chem.* **267**, 635–643.
20. Wright, S. D. & Meyer, B. C. (1986) *J. Immunol.* **136**, 1759–1764.
21. Garnier, J., Osguthorpe, D. J. & Robson, B. (1978) *J. Biol. Chem.* **120**, 97–120.
22. Arnaout, M. A. (1993) *Curr. Opin. Hematol.* **1**, 113–122.
23. Altieri, D. C., Bader, R., Mannucci, P. M. & Edgington, T. S. (1988) *J. Cell Biol.* **107**, 1893–1900.
24. Colombatti, A. & Bonaldo, P. (1991) *Blood* **77**, 2305–2315.
25. Lucchesi, B. R. & Mullane, K. M. (1986) *Annu. Rev. Pharmacol. Toxicol.* **26**, 201–224.